Arabian Journal for Science and Engineering (2023) 48:16281–16292
https://doi.org/10.1007/s13369-023-08145-5

RESEARCH ARTICLE-CHEMICAL ENGINEERING

Trimipramine Photo-Degradation in the Photo-Catalyst Baffled Reactor's UV/Sulfite/ZnO Redox Reaction System

Shohreh Azizi[1,2] · Maryam Sarkhosh[1,2,3] · Ilunga Kamika[4] · Touhami Mokrani[5] · Malik Maaza[1,2]

Received: 24 October 2022 / Accepted: 16 July 2023 / Published online: 12 August 2023

Abstract

The current work examines UV/Sulfite/ZnO (USZ) in reactor convectional (without baffles) and baffled photocatalytic reactors (BPCR) in order to cost-effectively photo-degrade trimipramine (TIR). The ideal conditions were 2:1:100 Sulfite/ZnO/TRI molar ratio, pH 7, and 30 min of reaction time for 97.4% TRI degradation. In the BPCR reactor, the measured rate constant (k_{obs}) and reaction rate (r_{obs}) both rise by around 17% and 50% as the TRI concentration is increased from 50 to 200 mgL^{-1}. The intermediate materials formed in three cases were examined by copper LC. Investigations showed that after 30 min, most of the intermediates became simple linear compounds such as hexane-1, 6-diol ($C_6H_{14}O_2$), formaldehyde (CH_2O), (E)-prop-1-en-1-yl-l2-azane (C_3H_6N), acetic acid $C_2H_4O_2$. Electrical energy consumption (E_{EO}) decreased from 8.61 $kWhm^3$ for convectional reactor to 5.37 $kWhm^3$ for BPCR due to an increase in k_{obs} and r_{obs}, for example, 200 mg L^{-1}. As a result, the total cost of the system (TCS) decreased from 3.56 for convectional reactor to 1.22 $ for PCBR reactor. According to information gathered, the UZS procedure lowers the BOD and COD levels by 66 to 86.29% in 80-min reaction time, respectively. Additionally, the BOD/COD ratio starts out at 0.26 and increases to 0.6 after 30 min.

Keywords Photo-degradation · Oxidative · Trimipramine · Reductive · Cost-effective

1 Introduction

Millions of individuals around the world suffer from mental disorders, including 23 million people with schizophrenia and other psychoses, 60 million people with bipolar disorder, and 300 million people who suffer from depression [1]. Pharmaceutical substances are effective for treating depression (APIs). APIs have unfortunately been found in surface and ground water, and they have attracted a lot of attention as "emerging" contaminants to be concerned about [2–4]. One of the major sources that contribute to the wastewater (WW) discharge of APIs is hospitals [5]. Health facilities are some significant sources of information because of the growing population and increase in psychiatric illnesses (HIs). However, typical WWTPs cannot filter water with trace levels of pharmaceutical contamination; as a result, the treatments used to remove it are unsuccessful [6]. Thus, they enter the aquatic system through the sediments and soil [7], surface and ground water [8], and even drinking and tap water [9] and can be detected there. Tricyclic antidepressant trimipramine (TRI, $C_{20}H_{26}N_2$), marketed under the brand name Surmontil, is prescribed to treat depression (TCA) Trimipramine has been found in hospital wastewater, the environment, and hospital wastewater treatment effluent [10]. For this reason, sophisticated oxidation reduction processes (AO/RPs) have arisen. The foundation of AORP's activity is on the generation of free radicals in order to break down contaminants

✉ Maryam Sarkhosh
Marya.sarkhosh@yahoo.com

1 UNESCO-UNISA Africa Chair in Nanosciences and Nanotechnology, College of Graduate Studies, University of South Africa, Muckleneuk Ridge, P.O. Box 392, Pretoria 0002, South Africa

2 Nanosciences African Network (NANOAFNET), iThemba LABS-National Research Foundation, 1 Old Faure Road, P.O. Box 722, Somerset West 7129, Western Cape, South Africa

3 Department of Environmental Health, School of Health, Mashhad University of Medical Sciences, Mashhad, Iran

4 Institute for Nanotechnology and Water Sustainability, School of Science, College of Science, Engineering and Technology, University of South Africa, Florida Campus, Johannesburg, South Africa

5 Department of Chemical Engineering, School of Engineering, University of South Africa, Private Bag X6, Florida 1710, South Africa

using the reactive radicals that are produced. A semiconductor photocatalyst can be used to accelerate the formation of radicals in the presence of an activating agent (e.g., UV radiation). The primary reasons zinc oxide (ZnO) is frequently used as a semiconductor photocatalyst are because it is nontoxic and economical. According to Eqs. (1) to (3), hydroxyl ions ($^{-}$OH) or water react with positive holes (h^+) to produce radicals called.$^{\bullet}$OH [11]

$$ZnO + h_\nu \rightarrow e_{aq}^- + h^+ \quad (1)$$

$$h^+ + H_2O \rightarrow H^+ + {}^{\bullet}OH \quad (2)$$

$$h^+ + {}^{-}OH \rightarrow {}^{\bullet}OH \quad (3)$$

Normally, reductive species including as I^- [12, 13], $SO_3{}^{2-}$ [14, 15], $CO_2{}^-$ [16] can be produced after UV light hits the anions in water. The study's use of Sulfite is due to high UV absorbance (εi, 254 = 220 M^{-1} cm^1) and electron generation per photon (eg, 0.286 mol E^{-1}); Sulfite is chosen in this study to generate the excessively reducing species according to Eqs. (4) to (7) [14].

$$SO_3^{2-} + h_\nu \rightarrow SO_3^{\bullet-} + e_{aq}^- \quad (4)$$

$$HSO_3^- + e_{aq}^- \rightarrow H^{\bullet} + SO_3^{\bullet-} \quad (5)$$

$$H^{\bullet} + H_2O \rightarrow H_3O^+ + e_{aq}^- \quad (6)$$

$$H^+ + e_{eq}^- \rightarrow H^{\bullet} \quad (7)$$

The duration and penetration depth for oxidative and reductive species in water are 6 mm and less than one second, respectively [15]. ZnO/NC nanocomposite ultrasonic catalysis can be used as a desirable treatment to clean up antibiotic-contaminated aquatic systems [16]. Electrochemically synthesized ZnO nanostructures have been successfully immobilized on powdered waste from the stone cutting industry and effectively used for catalytic destruction of a model anti-inflammatory pharmaceutical compound [17]. Additionally, the release of Sulfite and zinc oxide, which are the sources of reductive and oxidative species, causes the pollutants to degrade more quickly. The photocatalytic efficiency of eosin-TiO_2 when synthesized was significantly improved with the addition of $SO_3{}^{2-}$ [18]. The primary issues with AORPs are the excessive energy consumption and secondary pollution. These issues were resolved by the photo-catalyst baffled reactor (PCBR). Baffles were mounted on top of one another at an angle of 180 degrees to achieve a greater energy-efficient reactor. This creates rotational flow close to the UV light. In this study, simultaneous removal of an organic matter (Trimipramine) and a inorganic substance (Sulfite) was used. Broken down of organic matter by UV irradiation produces various radicals. Consequently, the fundamental purpose for this paper was to (1) assess the elimination of TIR by the reductive species generated with UV/Sulfite/ZnO process; (2) determine the effects of various operational parameters; (3) examine the reaction kinetic and energy consumption; (4) determine the intermediate by-products; (5) determine mineralization; (6) determine improvement of biodegradability.

2 Materials and Methods

2.1 Photo-Catalyst Baffled Reactor Configuration

As seen in Fig. 1, a UV lamp with a nominal power of 11 W and a light intensity of 78 W/cm^2 was utilized to provide UV radiation. A quartz sleeve was placed at a distance of 1 cm from the cylindrical glass. As a reaction space, TIR solution was injected into the open area between the quartz and cylindrical glass. A 500-mL container was used for the experiments. In this work, baffles were employed to shift the solution closest to the UV light in order to improve TIR degradation rate [19]. The baffles are cut in a corner and placed at an angle of 180 degrees. This type of placement of the baffles causes more movement of the liquid on the surface near the lamp. It is very important to consider the short penetration depth of 256-nm radiation in the degradation efficiency because it causes more UV rays to hit Sulfite ions, and as a result, more reducing species are produced. The baffles in the photoreactor were placed at an angle of 180 between each other to increase the mass transfer and interaction of UV rays with Sulfite ions in the reactor, which improved the removal efficiency and caused a significant reduction. This way of placing the baffles gave two advantages: 1 The liquid containing the pollutant and Sulfite anion gets closer to the UV radiation source; 2 circulating the liquid and thus exposing the entire liquid and mixing it in the reaction medium.

2.2 Analytical Methods

In order to ascertain the TRI concentration discovered using a high-performance liquid chromatograph (HPLC), by using the chemical oxygen demand (COD) test, which is used to inadvertently detect organic molecules, Eqs. (8–9) were utilized to calculate the rates of mineralization and destruction of TRI [20]

$$\text{TRI degradation} = \frac{\text{TRI}_0 - \text{TRI}_t}{\text{TRI}_0} \quad (8)$$

$$\text{TRI mineralization} = \frac{\text{CoD}_0 - \text{COD}_t}{\text{COD}_0} \quad (9)$$

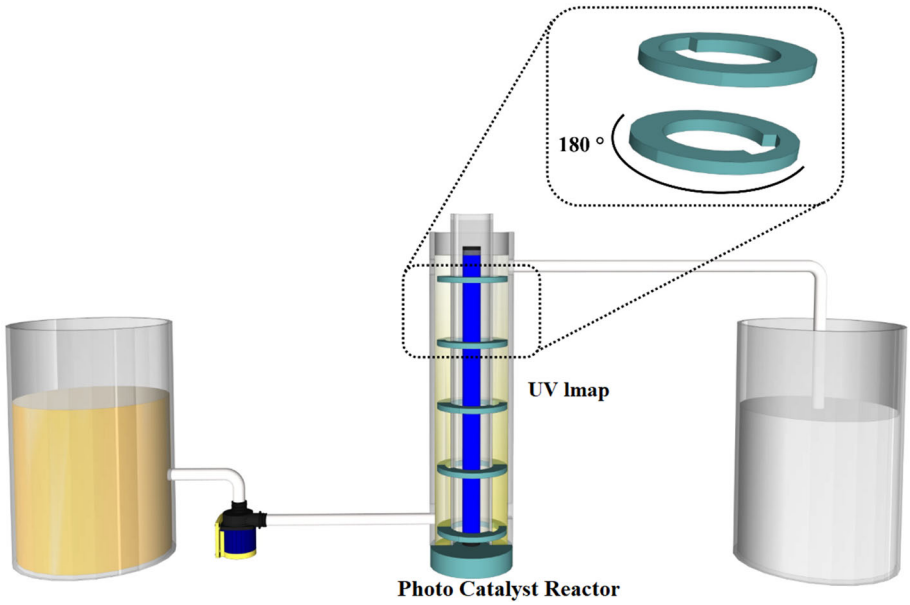

Fig. 1 Schematic of photo-catalyst baffled reactor

The biodegradability of different solutions can be confirmed with respect to their BOD_5/COD results or other combinations of their COD, BOD, and TOD levels. For instance, the average oxidation state (AOS) and carbon oxidation state (COS) parameters can be evaluated as the indicators of biodegradability. In this study, the biodegradability of the effluents was verified by calculating the values of these two indicators through Eqs. 10 and 11:

$$\mathrm{AOS} = 4 - 1.5\frac{\mathrm{CODt}}{\mathrm{TOCt}} \tag{10}$$

$$\mathrm{COS} = 4 - 1.5\,\frac{\mathrm{CODt}}{\mathrm{TOCi}} \tag{11}$$

where TOC is the TOC content of the treated TRI solutions (mg L^{-1}), COD is their COD content (mg L^{-1}), and the *i* and *t* subscripts, respectively, indicate their values at the beginning and time *t* of the UIZ process [19, 20]. After analysis of the biodegradability of the effluents, those with a BOD_5/COD ratio greater than 0.4 were proceeded to the biodegradation step (as a post-treatment). The chemical oxygen demand (COD) index was utilized to calculate the mineralization level. Samples containing CIP were measured for COD and biochemical oxygen demand (BOD) using the methods 5220B and 5210B described in the standard procedure (1). A CECILCE-4100 HPLC with UV detector (CE-4900) and C18 column (250 mm × 4.6 mm × 5 µm) was used to quantify TRI concentration. For TRI acetonitrile: acidic water (acetic acid 0.1 wt.%) (50:50, v/v) at 280 nm at a flow rate of 1.0 mL/min [20, 21], additionally, the impact of various anions on the TRI photo-degradation in the photo-reactor was examined. Additionally, LC-MS with ESI in the negative mode is employed to examine the TRI intermediates.

2.3 Kinetic Model, Energy, and Effective Cost Analyses

A pseudo-1st-order (PFO) kinetic model was used to investigate TRI photo-degradation in solutions and was implemented in accordance with Eqs. (12–13):

$$\ln\frac{C_t}{C_0} = -K_{\mathrm{obs}}\mathrm{t} \tag{12}$$

$$r_{\mathrm{obs}} = -k_{\mathrm{obs}}\mathrm{C}_{\mathrm{TRI}} \tag{13}$$

K is the constant response rate coefficient in this equation.

When selecting a treatment technique, important considerations including wastewater quality, economic, cost, etc., also play a significant influence. Electrical energy plays a significant role in operational expenses and is a substantial component of the cost of photoprocesses used to remove water contaminants. Despite the fact that there are numerous methods in the literature for calculating the AORP electrical energy consumption, which varies depending on the kind of pollutant, effluent quality, reactor configuration, and the type of source of light used, etc., it is essential to conduct an experimental study of the AORP electrical energy consumption. To calculate the amount of electrical energy (kWh) used in UV-based processes, the IUPAC proposed the parameter of energy used for each order (figure-of-merit), abbreviated E_{EO}. Electrical energy per order (E_{Eo}) E_{Eo} shows the total energy needed and enables quick calculation of electrical energy usage. E_{EO} values are used to compare the effectiveness of various processes' treatment strategies. This indicates that energy was required to photo-remove over 90% of the pollutants from a cubic meter of contaminated water [22].

$$IUPAC E_{EO} = \frac{P \times t \times 1000}{V \times 60 \times \log \frac{C_i}{C_f}} \quad (14)$$

P, V, and t in this equation stand for power (Kw), volume (L), and water's photo-reaction time (minutes), respectively. Equations (12) and (14) are combined and rearranged to produce a new E_{EO} based on the kinetic equation [23].

$$\text{Kinetic} E_{EO} = \frac{P \times 38.4}{V \times K_{\text{obs}}} \quad (15)$$

The anticipated values of E_{Eo} might be estimated using the IUPAC and kinetic model [23, 24]. Total cost of the system (TCS) ($\$ g^{-1}$) was also applied to cost-effective evaluation [25, 26]. For industrial customers, the global average price of electricity in 2020 is 0.121 US dollars per kWh.

$$\text{EEM} = \frac{Pt}{VM \times (c_i - c_e)} \quad (16)$$

$$\text{TCS} = 1.45\big(\text{EEM}\big(\text{k W h g}^{-1}\big) \times \text{Power cost}\big(\$/\text{k W h}\big) + \text{Oxidant cost}\big(\$\text{g}^{-1}\big)\text{Reductant cost}\big(\$\text{g}^{-1}\big)\big) \quad (17)$$

3 Results and Discussion

3.1 pH Role on TRI Photo-Degradation

There is investigation of TRI degradation with/without in various procedures. According to Fig. 2, only UV processes are significantly impacted by pH changes, while UV irradiation immediately breaks all bonds on the TRI structure (efficiency ranged from 12.7 to 13.7% and 22.87 to 21.03% in conventional and PCBR reactors, respectively). These data show that more than 80% more material is broken in the same time in the baffled reactor. While efficiency varied between 31.1 and 54.2% and 50.2 to 79.1% in conventional and PCBR reactors, respectively, solution pH had a substantial impact on TRI degradation in the UV/ZnO process. At an alkaline pH, the created positive holes (h^+) and the hydrogen ion (OH^-) (Eq. 3) rapidly react, resulting in the production of $OH^{\bullet}$. Additionally, TRI degradation in the UV/Sulfite process ranged from about 27 to 61.54% and in conventional and PCBR reactor and also from 42.3 to 74.04%, respectively. As is evident, pH changes have far less of an impact on the UV/Sulfite process. This was caused by the UV light's high efficiency of absorption (εi, 254 = 220 M^{-1} cm^{-1}), which also produced a lot of e_{aq}^- (e.g., 0.286 mol E^{-1} at 253.7 nm) [14]. The USZ process does not depend on the pH of the solution because of the high levels of eaq^- and $OH^{\bullet}$ r and other agents (efficiency ranged from 76.74 to 86.21% and 94.87 to 96.71% in traditional and PCBR reactors, respectively) [27]. It is crucial that the baffle is incorporated into the reactor's design to improve the TRI molecules' ability to degrade. This issue was evident in Mohseni et al., the CFD simulation, and the movement of the liquid, so near to the bulb is what caused it. This indicates that more pollutants will be immediately broken down and more reducing and oxidizing will be produced the closer the liquid (and the substance inside it) is to the light. The reaction rate consequently accelerates [28–30].

3.2 Impact of Molar Ratio on the UV/Iodide Process for TIR Photo-degradation

The findings of the investigation into the effects of various [Sulfite]/ [ZnO]/ [TRI] molar ratio in the USZ process (taking into account TIR concentration of 100 mg L^{-1}, pH 9, and reaction period 0 to 30 min) are shown in Fig. 3. According to Fig. 3, the maximum efficiency of around 100% for TIR was found at a 2:1 molar ratio between Sulfite and ZnO. The increase in efficiency varies based on the kind of contamination and is greatly reliant on whether it is proportionate to the bonds in the TIR molecule or the target molecule. Figure 3 depicts the pattern of TIR breakdown as the Sulfite and ZnO molar ratio changes. As can be observed, the removal effectiveness is higher in the 2:1 Sulfite: ZnO molar ratio than it is in other molar ratios. This is because the Sulfite: ZnO molar ratio plays an important role in the production of reducing and oxidative species. However, excessive increase can lead to Sulfite recombination and various other species that are much less effective (2). The key point is that when the Sulfite content is lower than the TIR, too much Sulfite reacts with these materials and is therefore not exposed to UV, resulting in significantly reduced e_{aq}^- production(3). These Sulfite derivatives can react with intermediate organic matter or TIR and be converted back to Sulfite. If the amount of Sulfite is lower than that of TIR, a significant amount of it will naturally be reacted with organic matter and the reaction with photons will be reduced, resulting in less reducing species such as e_{aq}^-(3). Based on Beer-Lambert's law, increasing the anion concentration due to increased UV adsorption leads to an increase in reactive species and thus better decomposition efficiency (4, 5). The result presented in this study is very similar to the study conducted by Jang et al. (6).

3.3 Kinetics, Energy, and Cost Analyses

Energy usage is a limiting constraint in the adoption of the AORPs procedure in terms of cost-effectiveness. In this work, photo-process energy consumption was calculated using the kinetic and IUPAC methods. The computed R^2 (0.95) in Table 1 shows that the pseudo-first-order (PFO) kinetics govern the TRI photo-degradation process. According to Fig. 4, the values of R^2 are calculated and provided in Table 1. The

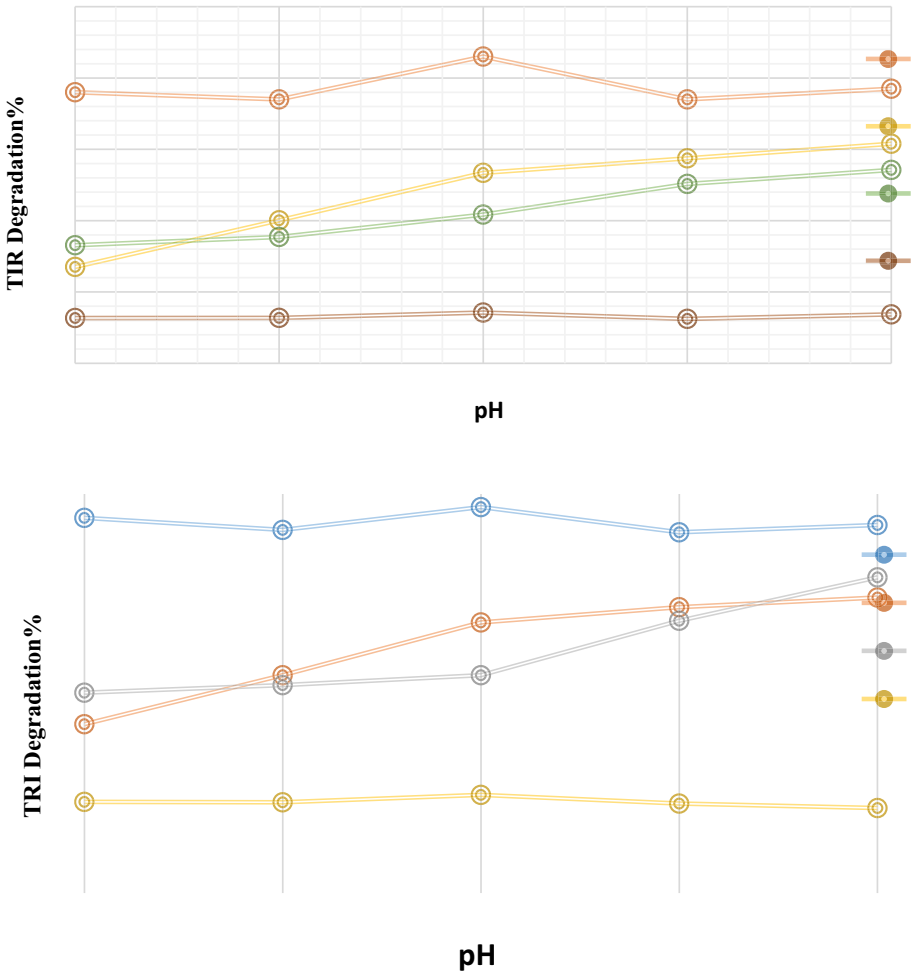

Fig. 2 The performance of (**a**) conventional, (**b**) BPCR reactor and the impact of pH on TRI degradation. The settings for the experiment were Sulfite: 1 mM, TRI: 100 mg L^{-1}, and a 30 minutes reaction duration

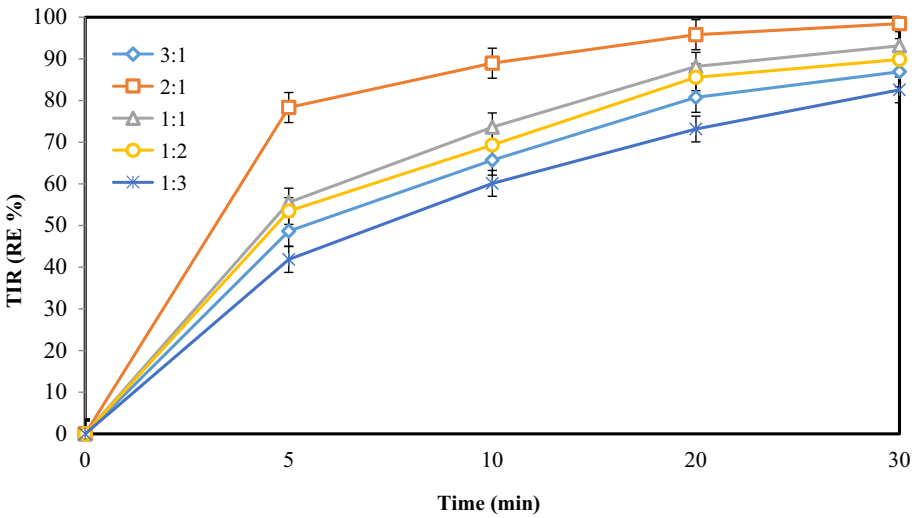

Fig. 3 Impact of Sulfite: ZnO molar ratio on TIR photo-degradation (reaction time = 30 min, pH = 7)

oxidizing and reducing species interacting with TRI caused the reaction rate to accelerate with concentration. Reaction constant k_{obs} and reaction rate r_{obs} of TRI degradation were directly impacted by TRI starting concentration [16, 27, 31]. In convectional and PCBR, respectively, k_{obs} ranges from 0.0748 to 0.0918 and from 0.0813 to 0.1218 (min^{-1}), whereas r_{obs} ranges from 3.74 to 18.36 and from 4.06 to 24.36 (mg L^{-1} min^{-1}). These data demonstrate that, firstly, k_{obs} and r_{obs} rise with increasing TRI concentration, and secondly, in the PCBR reactors compared to a conventional reactor, k_{obs}

Table 1 Data from the kinetics, energy, and total cost models

Type of reactor	Degradation-PFO						
	TRI (mg L^{-1})	R^2	K_{obs} (min^{-1})	r_{obs} (mg/L.min)	Kinetic E_{EO}(kwh/ /m3)	Figure-of-merit EEO(kwh /m3)	TCS ($ g − 1)
Convectional	50	0.9872	0.0748	3.74	15.23	12.66–17.41	12.54
PCBR	50	0.9723	0.0813	4.06	13.31	8.66–13.61	10.71
Convectional	100	0.9535	0.0791	7.01	12.53	9.81–14.77	9.12
PCBR	100	0.9814	0.1174	11.74	9.98	8.31–11.31	6.28
Convectional	200	0.9615	0.0918	18.36	8.61	7.26–10.15	3.56
PCBR	200	0.9672	0.1218	24.36	5.37	3.24–8.12	1.22

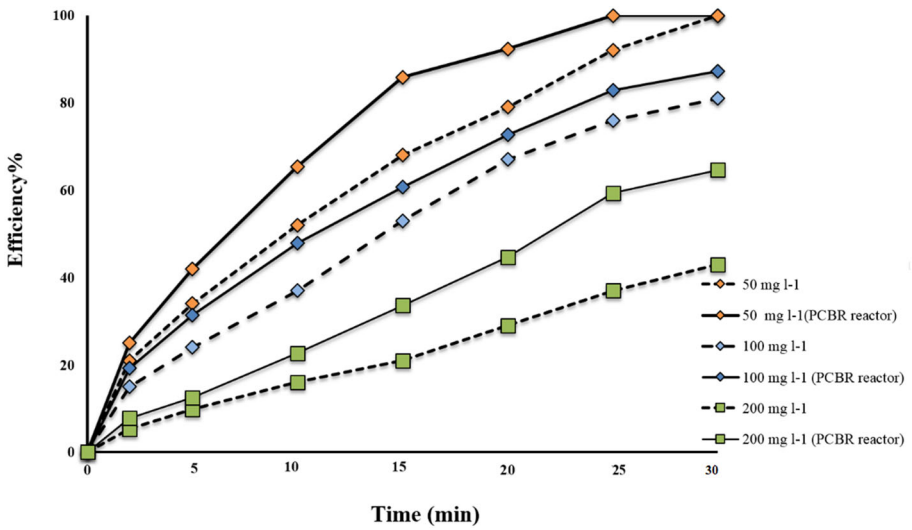

Fig. 4 Degradation efficiency versus time (conditions: pH 7 and fixed ratio of [Sulfite]/ [ZnO]/ [TRI] = 1:2:100)

increases by approximately 17% to 50% with increased TRI concentration from 50 and 200 mgL^{-1}, respectively. Additionally, r_{obs} in the convectional and PCBR reactors rises by around 4.9 and 6 times, respectively, with an increase in TRI concentration from 50 to 200 mg L^{-1}. Figure-of-merit E_{Eo} ranges from 12.66–17.41 to 7.26–10.15 $kWhm^3$ for convectional reactors and from 8.66–13.61 to 5.24–8.12 $kWhm^3$ when TRI concentration is increased from 50 to 200 mg L^{-1}, as shown in Table 1. Additionally, in the kinetic model, the E_{Eo} in the convectional and PCBR drops from 15.23 to 8.61 and from 13.31 to 5.37 kW h m^{-3}, respectively. As a result, the energy consumption in the PCBR reactor decreased by about 14% at 50 mg L^{-1} TRI concentration and by about 60% at 200 mg L^{-1} TRI concentration. The E_{Eo} value was in a different UV/Iodide/ZnO process research on 1 to 10 mgL^{-1} triclosan (2.48–12.29 kW h m^{-3}) [32]. Activated carbon photocatalyst is with TiO_2 coating for carbofuran breakdown (124.8 to 540.3 kW h m^{-3}) [33]. In many studies, energy usage rises as pollutants increase, while in certain studies, the contrary is true and energy consumption falls as pollutants rise in concentration [34, 35]. At various concentrations, the total cost of the system (TCS) was examined. PCBR reactors have lower TCS than conventional reactors, as indicated in Table 1. Additionally, the TCS falls as the TIR concentration and reaction rate rise.

3.4 The Effect of Anion in Water Matrix on TRI Degradation

The main anion found in surface and groundwater, which might come into contact with reactive species in AORPs and lessen their reactivity. To better study the interaction and competition of anions, their concentration was considered equal to the pollutant (100 mg L^{-1}). In the presence of nitrate anion, removal efficiency decreased from 100% in the presence of any anion to 78.85%. In the presence of NO_3^-, HCO_3^-, Cl^-, and SO_4^{2-}, respectively, TRI degradation decreases to 78.85%, 82.35%, 89.28%, and 94.94% in Fig. 4. Onion UV absorption and the production of anionic radicals result in less TRI breakdown. Additionally, NO_3^-

has a stronger impact than other anion due to its higher acid dissociation constant (ka) [36].

$$HCO_3^- + {}^{\bullet}HO \rightarrow CO_3^{\cdot -} + H_2O \quad (18)$$

$$Cl^- + {}^{\bullet}HO \rightarrow ClOH^{\bullet -} \quad (19)$$

$$NO_3^- + {}^{\bullet}HO \rightarrow NO_3^{\bullet} + OH^- \quad (20)$$

$$SO_4^{2-} + {}^{\bullet}HO \rightarrow SO_4^{\bullet -} + OH^- \quad (21)$$

$$HCO_3^- + e_{aq}^- \rightarrow HCO_3^{2-} \quad (22)$$

$$Cl^- + e_{aq}^- + H^+ \rightarrow HCl \quad (23)$$

$$NO_3^- + e_{aq}^- \rightarrow (NO_3)^{\bullet 2-} \quad (24)$$

$$SO_4^{2-} + e_{aq}^- \rightarrow SO_4^{3-} \quad (25)$$

The effect of nitrate is larger because it has a higher acid solubility constant (ka) than any other anion [36]. In addition, it should be attributed to the fact that the TIR molecule contains N atoms, where the N atom in TIR is oxidized to NO_3 by the action of $^{\bullet}OH$ radicals, as seen in Eq. (26) [37]. Following the equilibrium law (Le Chatelier's), the produced $NO_3{}^-$ may reduce the TIR photo-degradation efficiency.

$$C_{18}H_{20}FN_3O_4 + {}^{\bullet}HO \rightarrow NO_3^- + \text{products} \quad (26)$$

Additionally, the primary inference mechanism for nitrate reduction is that nitrate undergoes a reaction with the generated electron and is converted to nitrogen gas in two steps: Nitrate is reduced by an electron to nitrogen gas (N_2) [38].

$$NO_3^- + 5\,e_{aq}^- + 6H^+ \rightarrow N_2(g) + 3\,H_2O \quad (27)$$

Nitrate reduction to nitrite and nitrite reduction to N_2 are the two components of this process.

$$NO_3^- + 2\,e_{aq}^- + 2H^+ \rightarrow 2NO_2^- + H_2O \quad (28)$$

$$NO_3^- + 3\,e_{aq}^- + 4H^+ \rightarrow N_2(g) + 2\,H_2O \quad (29)$$

3.5 TRI Intermediate and Degradation Pathways

By taking a sample of the reactor's effluent after a 30-min reaction time, the manufacturing intermediates in the USZ process's TRI breakdown were studied. The LC–MS with ESI in the negative mode is employed to examine the TRI intermediates. Within 5.1 min and 295.20 m/z of retention time, the molecular ion for TRI was visible. Eight intermediates in total, as shown in Table 2, were found. A potential TRI breakdown mechanism was hypothesized based on the intermediates found, and it is shown in Figs. 5 and 6. The initial TRI degradation can occur in four different ways (Fig. 7). A C–C breaking band is followed by a C = C breaking band, a C = C conversion to a C–C, and an N–C breaking band. TRI hydrolysis (I_1–I_3) or TRI ring breaking to two halves occurs in the first stage (I_4-I_6). The TRI molecules are broken down by both $e_{aq}{}^-$ and $^{\bullet}OH$. The fluoride atom stings the benzene ring due to its strong electronegativity, and detaching it with eaq significantly aids in breaking the ring [14, 39]. The compounds with a high capacity to complete mineralization such as hexane-1,6-diol ($C_6H_{14}O_2$), formaldehyde (CH_2O), (E)-prop-1-en-1-yl-l2-azane (C_3H_6N), acetic acid $C_2H_4O_2$ were generated in the third phase (COD lowering) (I_7-I_9) and then to CO_2, H_2O, $NH_4{}^+$, and NH_3. In 30 min, no substance was detected, which of course could be due to a decrease in the concentration of intermediate substances or a decrease in the carbon content that was not detected by the device.

3.6 USZ-Based TRI Mineralization and Biodegradability

When organic materials are mineralized to reduce pollution, very stable inorganic chemicals including water, carbon dioxide, and salt are created. At 100 mg L^{-1} TRI, under ideal conditions, the TRI mineralization is studied. COD and TOC levels in the effluent of the USZ process were measured to ascertain the extent of mineralization. Within an 80-min photoreaction, the USZ technique lowers the BOD and COD levels by 66% and 86.29%, respectively. However, due to the high energy consumption at this period and the need for 80 min for 86% of mineralization, despite the fact that BOD/COD ratio starts off at 0.26 and increases to 0.6 after 30 min of photoreaction, the BOD/COD value was in a different UV/Iodide/ZnO process research on 10 mgL^{-1} triclosan (0.57 to 0.66). The BOD/COD ratio for triclosan is the rapid consumption of linear materials, as well as the need to convert some of the ring-shape structures to linear constituent [32]. As a result, this reactor can be used to degrade persistent organic pollutants (POP_s) and emerging contaminants (ECs) in aqueous medium and then enter the resulting effluent into the biological reactor. This method reduces the toxicity of drugs, and microorganisms are able to completely decompose them as a carbon source. A biological reactor after a photocatalytic reactor (after 30 min) will help mineralize all metabolites, because the researchers said that biodegradation is a recommended method for mineralizing biodegradable organic compounds [40].

Table 2 Intermediates explored in TRI photo-degradation

Intermediates symbol	Photoreaction time (min)	Retention time (min)	Detected mass (m/z)	Molecular weight	Chemical formula	Molecular name	Reported in other AO/RPs
I_1	10	5.1	295.21	294.44	$C_{20}H_{26}N_2$	3-(10,11-Dihydro-5H-dibenzo[b,f]azepin-5-yl)-N,N,2-trimethylpropan-1-amine	YES
I_2	10	3.7	196.11	195.27	$C_{14}H_{13}N$	10,11-Dihydro-5H-dibenzo[b,f]azepine	No
I_3	10	7.4	287.24	286.46	$C_{19}H_{30}N_2$	N1-(2-ethylphenyl)-N3,N3,2-trimethyl-N1-((1E,3Z)-penta - 1,3-dien-1-yl)propane-1,3-diamine	No
I_4	10	5.2	262.25	261.45	$C_{18}H_{31}N$	5-butyl-2,3,4,4a,5,5a,6,7,8,10,11,11a-Dodecahydro-1H-dibenzo[b,f]azepine	YES
I_5	10	5.7	285.23	284.45	$C_{19}H_{28}N_2$	(Z)-3-(3-Ethylidene-2-methylene-2,3,4,5-tetrahydro-1H-benzo [b]azepin-1-yl)-N,N,2-trimethylpropan-1-amine	No
I_6	10	12.8	261.23	260.43	$C_{17}H_{28}N_2$	N1,N1,2-trimethyl-N3-(2-propylphenyl)-N3-vinylpropane-1,3-diamine	No
I_7	15	4.1	157.18	156.29	$C_{10}H_{22}N$	(4-Ethylheptan-3-yl)(methyl)-l2-azane	YES
I_8	15	5.8	299.34	298.56	$C_{19}H_{42}N_2$	N1,N1,2-trimethyl-N3-octyl-N3-pentylpropane-1,3-diamine	No
I_9	15	7.1	139.14	138.25	$C_{10}H_{18}$	(2E,6E)-deca-2,6-diene	YES
I_{10}	15	12.9	211.23	210.39	$C_{14}H_{28}N$	Butyl(2-butylcyclohexyl)-l2-azane	No
I_{11}	15	**7.7**	231.18	230.36	$C_{15}H_{22}N_2$	N-(3-(l1-azaneyl)-2-methylpropyl)-2-propyl-N-vinylaniline	No
I_{12}	15	**6.7**	119.10	118.18	$C_6H_{14}O_2$	hexane-1,6-diol	YES
I_{13}	20	7.2	47.01	46.03	CH_2O_2	Formic acid	YES
I_{14}	20	4.9	31.01	30.03	CH_2O	Formaldehyde	YES
I_{15}	20	12.5	57.05	56.09	C_3H_6N	(E)-prop-1-en-1-yl-l2-azane	No
I_{16}	20	7.4	61.02	60.05	$C_2H_4O_2$	Acetic acid	YES

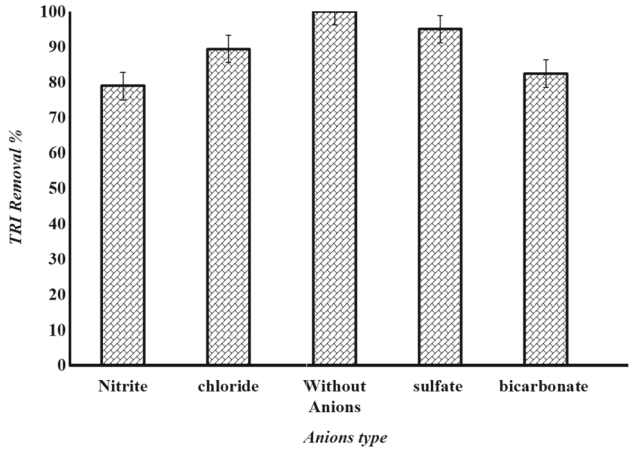

Fig. 5 Anions effect on 100 mg $L.^{-1}$ TRI degradation (pH = 7, reaction time = 30 min, Sulfite /ZnO/TRI molar ratio = 2:1:100)

4 Conclusions

Numerous health issues caused by organic solvent-resistant matter to biodegradation have forced communities to utilize cutting-edge techniques to address them. Additionally, the utilization of nanoparticle-based technologies (such as adsorption or advanced oxidation) would result in the production of a secondary pollutant; therefore, worries regarding their existence cannot be disregarded. The purpose of this study is to investigate the effectiveness of the advanced UV/Sulfite/ZnO redox reaction system in improving the biological degradability of wastewater containing the antibiotic TRI. Also, the baffles are cut in a corner and placed at an angle of 180 degrees. This type of placement of the baffles causes more movement of the liquid on the surface near the lamp. It is very important to consider the short penetration depth of 256-nm radiation in the degradation efficiency because it causes more UV rays to hit Sulfite ions, and as

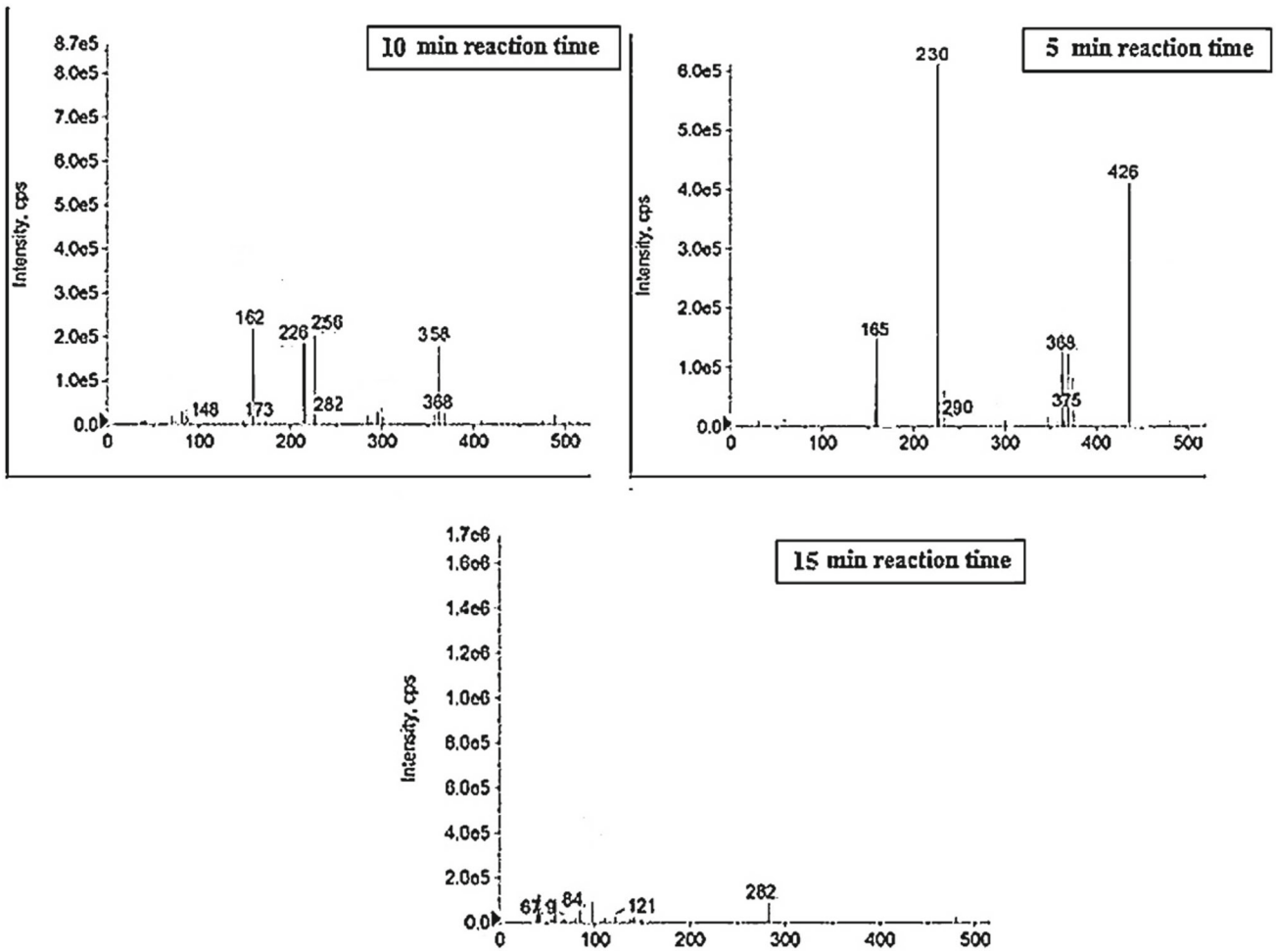

Fig. 6 LC/MS chromatograms of the USZ process effluent in the negative ESI mode (pH = 7, reaction time = 10 to 30 min, Sulfite /ZnO/TRI molar ratio = 2:1:100)

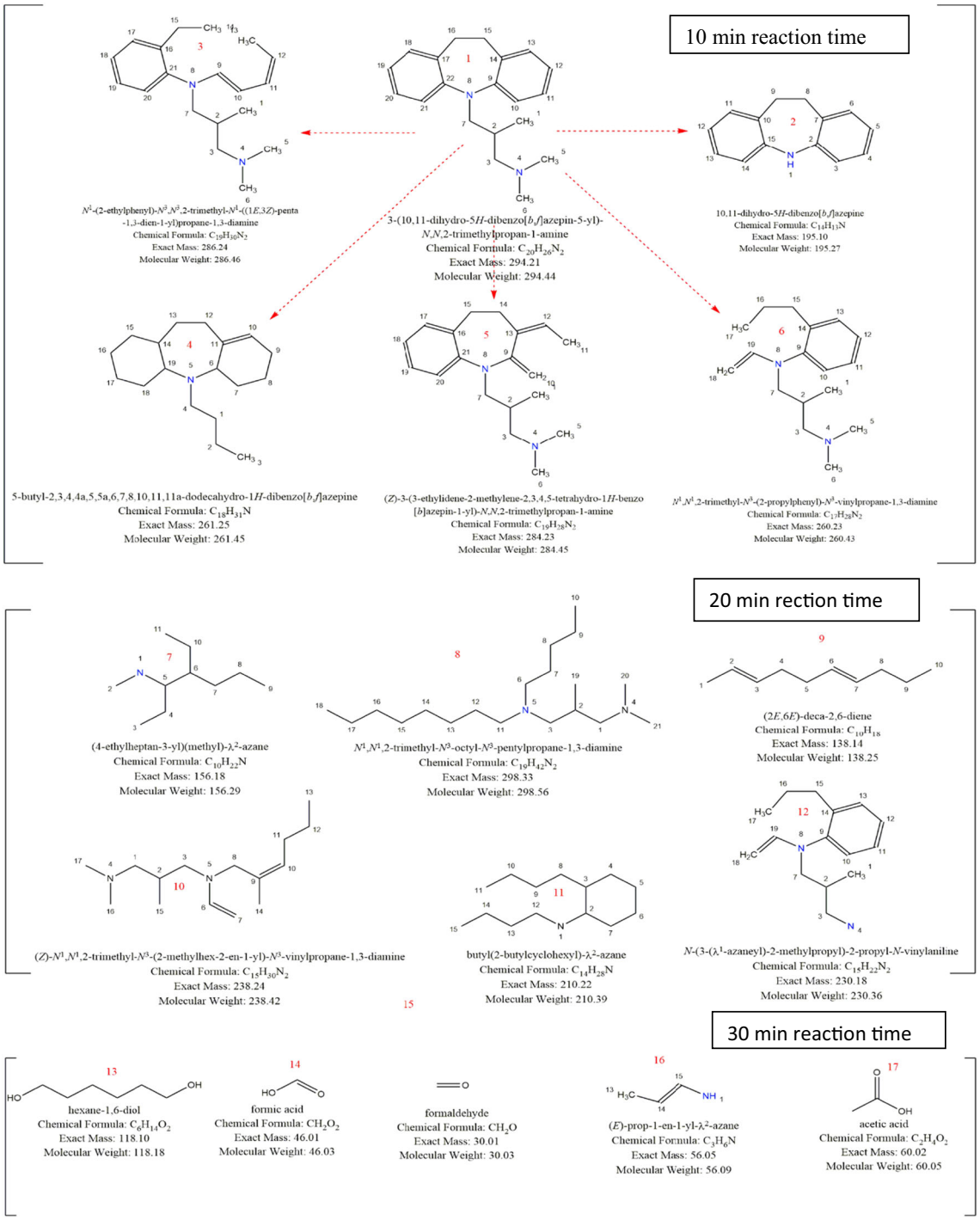

Fig. 7 TRI intermediates in the USZ treatment process (pH = 7, reaction time = 10 to 30 min, Sulfite /ZnO/TRI molar ratio = 2:1:100)

a result, more reducing species are produced. The baffles in the photoreactor were placed at an angle of 180 between each other to increase the mass transfer and interaction of UV rays with Sulfite ions in the reactor, which improved the removal efficiency and caused a significant reduction. This way of placing the baffles gave two advantages: 1 The liquid containing the pollutant and Sulfite anion gets closer to the UV radiation source; 2 circulating the liquid and thus exposing the entire liquid and mixing it in the reaction medium. The kinetics of the reaction was investigated by the pseudo-first-order model method, and the reaction constant and reaction rate decreased with increasing concentration. The energy consumption was calculated by kinetic and IUPAC methods, which shows that in both models, the

amount of energy consumption increased with increasing concentration. The effect of the main water anions on the performance of the UV/Sulfite/ZnO redox reaction system was investigated, and the most negative effect on the process was found for nitrate, bicarbonate, sulfate, and chloride. Reactive species were investigated using scavengers, and reducing species (hydrated electrons, hydrogen radicals) played an key roles in the photo-degradation of pollutants. By examining the intermediate compounds identified, it was found that the cyclic compounds have been transformed into linear and simple organic and rapidly biodegradable compounds. Within an 80-min photoreaction, the USZ technique lowers the BOD and COD levels by 66% and 86.29%, respectively. Despite the fact that BOD/COD ratio starts off at 0.26 and increases to 0.6 after 30 min of photoreaction. As a consequence of this work, it is now possible to treat wastewater containing refractory organic materials, such as TRI, in an effective and ecologically beneficial manner by using a biological process that comes after the ARP procedure.

Funding Open access funding provided by University of South Africa. The authors did not receive support from any organization for the submitted work.

Declarations

Conflict of interest The authors declare that there is no conflict of interest for this paper. The authors declare they have no financial interests.

References

1. Loveys, K.; Niederhoffer, K.; Prud'hommeaux, E.; Resnik, R. & Resnik, P. In *Proceedings of the fifth workshop on computational linguistics and clinical psychology: from keyboard to clinic.*
2. Ahkola, H., et al.: Presence of active pharmaceutical ingredients in the continuum of surface and ground water used in drinking water production. Environ. Sci. Pollut. Res. **24**, 26778–26791 (2017)
3. Allijn, I.E.; Oldenkamp, R.; Storm, G.; Ragas, A.M.; Schiffelers, R.M.: Environmental impact of switching from the synthetic glucocorticoid prednisolone to the natural alkaloid berberine. PLoS ONE **13**, e0199095 (2018)
4. Williams, M., et al.: Emerging contaminants in a river receiving untreated wastewater from an Indian urban centre. Sci. Total Environ. **647**, 1256–1265 (2019)
5. Schuster, A.; Hädrich, C.; Kümmerer, K.: Flows of active pharmaceutical ingredients originating from health care practices on a local, regional, and nationwide level in Germany—is hospital effluent treatment an effective approach for risk reduction? Water Air Soil Pollut. Focus **8**, 457–471 (2008)
6. Teixeira, S., et al.: Photocatalytic degradation of pharmaceuticals present in conventional treated wastewater by nanoparticle suspensions. J. Environ. Chem. Eng. **4**, 287–292 (2016)
7. Li, W.C.: Occurrence, sources, and fate of pharmaceuticals in aquatic environment and soil. Environ. Pollut. **187**, 193–201 (2014)
8. Jones, O.; Voulvoulis, N.; Lester, J.: Aquatic environmental assessment of the top 25 English prescription pharmaceuticals. Water Res. **36**, 5013–5022 (2002)
9. Fram, M.S.; Belitz, K.: Occurrence and concentrations of pharmaceutical compounds in groundwater used for public drinking-water supply in California. Sci. Total Environ. **409**, 3409–3417 (2011)
10. Doll, T.E.; Frimmel, F.H.: Fate of pharmaceuticals—photodegradation by simulated solar UV-light. Chemosphere **52**, 1757–1769 (2003)
11. Mou, H.; Song, C.; Zhou, Y.; Zhang, B.; Wang, D.: Design and synthesis of porous Ag/ZnO nanosheets assemblies as super photocatalysts for enhanced visible-light degradation of 4-nitrophenol and hydrogen evolution. Appl. Catal. B **221**, 565–573 (2018)
12. Azarpira, H., et al.: Photo-catalytic degradation of triclosan with UV/Iodide/ZnO process: performance, kinetic, degradation pathway, energy consumption and toxicology. J. Photochem. Photobiol. A Chem.. **371**, 423 (2018)
13. Sun, Z.; Zhang, C.; Chen, P.; Zhou, Q.; Hoffmann, M.R.: Impact of humic acid on the photoreductive degradation of perfluorooctane sulfonate (PFOS) by UV/Iodide process. Water Res. **127**, 50–58 (2017)
14. Yazdanbakhsh, A.; Eslami, A.; Moussavi, G.; Rafiee, M.; Sheikhmohammadi, A.: Photo-assisted degradation of 2, 4, 6-trichlorophenol by an advanced reduction process based on sulfite anion radical: degradation, dechlorination and mineralization. Chemosphere **191**, 156–165 (2018)
15. Xie, B., et al.: One-step removal of Cr (VI) at alkaline pH by UV/sulfite process: reduction to Cr (III) and in situ Cr (III) precipitation. Chem. Eng. J. **308**, 791–797 (2017)
16. Liu, X., et al.: Trichloroacetic acid reduction by an advanced reduction process based on carboxyl anion radical. Chem. Eng. J. **303**, 56–63 (2016)
17. Attri, P., et al.: Generation mechanism of hydroxyl radical species and its lifetime prediction during the plasma-initiated ultraviolet (UV) photolysis. Sci. Rep. **5**, 9332 (2015)
18. Bagheri, M.; Mohseni, M.: A study of enhanced performance of VUV/UV process for the degradation of micropollutants from contaminated water. J. Hazard. Mater. **294**, 1–8 (2015)
19. Moussavi, G.; Pourakbar, M.; Shekoohiyan, S.; Satari, M.: The photochemical decomposition and detoxification of bisphenol a in the VUV/H_2O_2 process: degradation, mineralization, and cytotoxicity assessment. Chem. Eng. J. **331**, 755–764 (2018)
20. Murcia-López, S.; Villa, K.; Andreu, T.; Morante, J.R.: Improved selectivity for partial oxidation of methane to methanol in the presence of nitrite ions and BiVO 4 photocatalyst. Chem. Commun. **51**, 7249–7252 (2015)
21. Chu, C.-Y.; Huang, M.H.: Facet-dependent photocatalytic properties of Cu_2 O crystals probed by using electron, hole and radical scavengers. J. Mater. Chem. A **5**, 15116–15123 (2017)
22. Rasolevandi, T.; Naseri, S.; Azarpira, H.; Mahvi, A.: Photodegradation of dexamethasone phosphate using UV/Iodide process: Kinetics, intermediates, and transformation pathways. J. Mol. Liq. **295**, 111703 (2019)

23. Lee, C.-G., et al.: Porous electrospun fibers embedding TiO2 for adsorption and photocatalytic degradation of water pollutants. Environ. Sci. Technol. **52**, 4285 (2018)
24. Rasolevandia, T.; Azarpirab, H.; Mahvia, A.H.: Modeling and optimizing chromate photo-precipitation with iodide exciting under UV irradiation. Desalin. Water Treat. **195**, 369–376 (2020)
25. Dhaka, S.; Kumar, R.; Lee, S.-H.; Kurade, M.B.; Jeon, B.-H.: Degradation of ethyl paraben in aqueous medium using advanced oxidation processes: efficiency evaluation of UV-C supported oxidants. J. Clean. Prod. **180**, 505–513 (2018)
26. Xu, Y.; Lin, Z.; Zhang, H.: Mineralization of sucralose by UV-based advanced oxidation processes: UV/PDS versus UV/H_2O_2. Chem. Eng. J. **285**, 392–401 (2016)
27. Moradi, M.; Moussavi, G.: Investigation of chemical-less UVC/VUV process for advanced oxidation of sulfamethoxazole in aqueous solutions: evaluation of operational variables and degradation mechanism. Sep. Purif. Technol. **190**, 90–99 (2018)
28. Duran, J.E.; Taghipour, F.; Mohseni, M.: CFD modeling of mass transfer in annular reactors. Int. J. Heat Mass Transf. **52**, 5390–5401 (2009)
29. Duran, J.E.; Mohseni, M.; Taghipour, F.: Modeling of annular reactors with surface reaction using computational fluid dynamics (CFD). Chem. Eng. Sci. **65**, 1201–1211 (2010)
30. Bagheri, M.; Mohseni, M.: Pilot-scale treatment of 1, 4-dioxane contaminated waters using 185 nm radiation: experimental and CFD modeling. J. Water Process Eng. **19**, 185–192 (2017)
31. Moussavi, G.; Rezaei, M.: Exploring the advanced oxidation/reduction processes in the VUV photoreactor for dechlorination and mineralization of trichloroacetic acid: Parametric experiments, degradation pathway and bioassessment. Chem. Eng. J. **328**, 331–342 (2017)
32. Azarpira, H., et al.: Photo-catalytic degradation of triclosan with UV/iodide/ZnO process: performance, kinetic, degradation pathway, energy consumption and toxicology. J. Photochem. Photobiol., A **371**, 423–432 (2019)
33. Vishnuganth, M.; Remya, N.; Kumar, M.; Selvaraju, N.: Photocatalytic degradation of carbofuran by TiO_2-coated activated carbon: model for kinetic, electrical energy per order and economic analysis. J. Environ. Manage. **181**, 201–207 (2016)
34. Xiao, Q., et al.: An overview of advanced reduction processes for bromate removal from drinking water: reducing agents, activation methods, applications and mechanisms. J. Hazard. Mater. **324**, 230–240 (2017)
35. Moussavi, G.; Jiani, F.; Shekoohiyan, S.: Advanced reduction of Cr (VI) in real chrome-plating wastewater using a VUV photoreactor: batch and continuous-flow experiments. Sep. Purif. Technol. **151**, 218–224 (2015)
36. Rahmah, A.; Harimurti, S.; Murugesan, T.: Experimental investigation on the effect of wastewater matrix on oxytetracycline mineralization using UV/H_2O_2 system. Int. J. Environ. Sci. Technol. **14**, 1225–1233 (2017)
37. Bianco Prevot, A., et al.: Photocatalytic degradation of acid blue 80 in aqueous solutions containing TiO_2 suspensions. Environ. Sci. Technol. **35**, 971–976 (2001)
38. Moussavi, G.; Shekoohiyan, S.: Simultaneous nitrate reduction and acetaminophen oxidation using the continuous-flow chemical-less VUV process as an integrated advanced oxidation and reduction process. J. Hazard. Mater. **318**, 329–338 (2016)
39. Sarkhosh, M., et al.: Enhancing photo-degradation of ciprofloxacin using simultaneous usage of eaq− and OH over UV/ZnO/I-process: efficiency, kinetics, pathways, and mechanisms. J. Hazard. Mater. **377**, 418–426 (2019)
40. Aghapour, A.A.; Moussavi, G.; Yaghmaeian, K.: Degradation and COD removal of catechol in wastewater using the catalytic ozonation process combined with the cyclic rotating-bed biological reactor. J. Environ. Manage. **157**, 262–266 (2015)